Caged-Iron Chelators a Novel Approach towards Protecting Skin Cells against UVA-Induced Necrotic Cell Death

Anthie Yiakouvaki[1,3], Jelena Savović[1,3], Abdullah Al-Qenaei[1], James Dowden[2] and Charareh Pourzand[1]

Exposure of human skin cells to solar UVA radiation leads to an immediate dose-dependent increase of labile iron that subsequently promotes oxidative damage and necrotic cell death. Strong iron chelators have been shown to suppress cell damage and necrotic cell death by moderating the amount of labile iron pool (LIP), but chronic use would cause severe side effects owing to systemic iron depletion. Prodrugs that become activated in skin cells at physiologically relevant doses of UVA, such as "caged-iron chelators", may provide dose- and context-dependent release. Herein, we describe prototypical iron chelator compounds derived from salicylaldehyde isonicotinoyl hydrazone and pyridoxal isonicotinoyl hydrazone and demonstrate that the intracellular LIP and subsequent necrotic cell death of human skin fibroblasts is significantly decreased upon exposure to a combination of the prototypical compounds and physiologically relevant UVA doses. Iron regulatory protein bandshift and calcein fluorescence assays reveal decreased intracellular LIP following irradiation of caged-chelator-treated cells, but not in control samples where either UVA light, or caged-chelator is absent. Furthermore, flow cytometry shows that these compounds have no significant toxicity in the skin fibroblasts. This novel light-activated prodrug strategy may therefore be used to protect skin cells against the deleterious effects of sunlight.

Journal of Investigative Dermatology (2006) **126,** 2287–2295. doi:10.1038/sj.jid.5700373; published online 18 May 2006

INTRODUCTION

There is significant interest in understanding and controlling the cellular mechanisms that cause skin damage upon prolonged exposure to the UV component of sunlight. It is now known that UVA radiation of skin cells leads to an immediate release of labile iron (Pourzand *et al.*, 1999) and susceptibility to both oxidative membrane damage and necrotic cell death owing to a loss of plasma membrane integrity, presumably as a result of iron-catalyzed biological oxidation (Reelfs *et al.*, 2004; Zhong *et al.*, 2004). Damage owing to further exposure to UVA is likely to be further exacerbated as a result (Zhong *et al.*, 2004).

Normally, the cellular labile iron pool (LIP) (see, Kakhlon and Cabantchik, 2002) is tightly regulated (Breuer *et al.*, 1996; Epsztejn *et al.*, 1997; Cairo and Pietrangelo, 2000; Petrat *et al.*, 2001) by cytosolic iron regulatory proteins 1 and 2 (IRPs) (Beinert and Kennedy, 1993; Klausner *et al.*, 1993; Kuhn, 1994; Guo *et al.*, 1995; Hentze and Kuhn, 1996), but pathological conditions that severely alter iron homeostasis (Cairo *et al.*, 1995, 1996; Martins *et al.*, 1995; Pantopoulos and Hentze, 1995; Pourzand *et al.*, 1999) lead to enhanced oxidative cell injury.

Iron chelation offers a simple method of rectifying unbalanced iron levels. Bisset *et al.* (1991) emphasized the importance of topical iron chelators to protect skin cells against the UV-induced increase in skin iron. Strong iron chelators such as desferrioxamine mesylate (DFO) suppress both cell damage (Zhong *et al.*, 2004) and iron release (Pourzand *et al.*, 1999; Kvam *et al.*, 2000; Reelfs *et al.*, 2004; Zhong *et al.*, 2004) induced by UVA. Unfortunately, prolonged dosing with exposure to strong iron chelators leads to side effects as a result of the removal of essential iron from various sites including iron-containing enzymes (Porter and Huens, 1989; Singh *et al.*, 1995; Hileti *et al.*, 1995; Rakba *et al.*, 2000; Simonart *et al.*, 2000). To minimize these sides effects, a series of photoprotective iron chelation strategies have been proposed in oxidative conditions (Galey *et al.*, 2000; Séité *et al.*, 2004). Alternatively, design of mild

[1]*Department of Pharmacy and Pharmacology, University of Bath, Claverton Down, Bath, UK and* [2]*Centre for Biomolecular Sciences, School of Chemistry, University of Nottingham, University Park, Nottingham, UK*

[3]*These authors contributed equally to this work.*

Correspondence: Dr Charareh Pourzand, Department of Pharmacy and Pharmacology, University of Bath, Claverton Down, Bath, BA2 7AY, UK. E-mails: prscap@bath.ac.uk or james.dowden@nottingham.ac.uk

Abbreviations: BIH, isonicotinic acid benzylidene-hydrazide; BnSIH, isonicotinic acid (2-benzyloxy-benzylidene)-hydrazide; CA, calcein; CA-AM, calcein acetoxymethyl ester; CA-Fe, CA-bound iron; DFO, desferrioxamine mesylate or Desferal; DMSO, dimethyl sulfoxide; FAB, fast atom bombardment; Ft, ferritin; IRE, iron-responsive element; IRP, iron regulatory protein; K_d, dissociation constant; LIP, labile iron pool; 2-NPE-PIH, (2-nitrophenyl)ethyl pyridoxal isonicotinoyl hydrazone; 2-NPE-SIH, (2-nitrophenyl)ethyl salicylaldehyde isonicotinoyl hydrazone; NMR, nuclear magnetic resonance; PI, propidium iodide; PIH, pyridoxal isonicotinoyl hydrazone; RT, room temperature; ROS, reactive oxygen species; SIH, salicylaldehyde isonicotinoyl hydrazone; TfR, transferrin receptor

Received 4 January 2006; revised 15 March 2006; accepted 16 March 2006; published online 18 May 2006

chelators (Kitazawa *et al.*, 2005) have been reported to reduce considerably the observed toxic side effects by strong chelators such as induction of hypoxia-inducing factor-1, as demonstrated in a study by Creighton-Gutteridge and Tyrrell (2002).

We envisaged that caged iron chelators, rendered inactive by a photolabile protecting group that is later released upon exposure to UV irradiation, would potentially reduce side effects arising from chronic exposure to iron chelators. Under normal conditions, such compounds would have low affinity for iron and become dispersed within skin cells without causing iron starvation. However, photolysis (UVA radiation) would furnish the highly potent uncaged chelator capable of effective chelation and removal of the UVA-induced labile iron. Simple prototypical compounds derived from strong iron chelators salicylaldehyde isonicotinoyl hydrazone (SIH) and pyridoxal isonicotinoyl hydrazone (PIH), elaborated with the 1-(2-nitrophenyl)ethyl (2-NPE) caging group (Figure 1), were thus synthesized. Both SIH and PIH are Fe(III)-specific tridentate ligands that chelate iron as effectively as DFO and are powerful inhibitors of iron-dependent production of hydroxyl radicals from hydrogen peroxide, mitochondrial lipid peroxidation, and other oxidative injuries as demonstrated in a series of cellular and animal studies (Hershko *et al.*, 1981; Richardson and Ponka, 1998; Hermes-Lima *et al.*, 1999; Horackova *et al.*, 2000; Santos *et al.*, 2001; Chaston and Richardson, 2003; Buss *et al.*, 2003a; Šimunek *et al.*, 2005). Additionally, hydrophilic iron chelators, such as DFO, are poorly cell permeant, whereas lipophilic PIH and SIH efficiently enter cells and tissues (Ponka *et al.*, 1979, 1994; Huang and Ponka, 1983; Epsztejn *et al.*, 1997). The chelator SIH is sufficiently lipophilic to readily cross the cell membrane and even transport iron (i.e. redox-inactive iron) to the extracellular media.

To test this concept, caged iron chelators were examined for (i) ''uncaging'' by broad-spectrum UVA radiation at a physiological relevant dose; (ii) iron chelation by caged and uncaged products *in vitro*; (iii) modulation of the intracellular labile iron concentration before, and following UVA-irradiation of a human skin fibroblast cell line, FEK4; and (iv) protection of skin cells from oxidative damage following radiation treatment. Our results demonstrate that unlike the parent compounds, the caged iron chelators do not diminish the normal LIP in cells, until exposure to a physiologically relevant UVA dose when they subsequently provide promising levels of protection for skin fibroblast cells against UVA-mediated necrotic cell death.

RESULTS

Chemistry: synthesis of caged compounds and analogues

The phenol group is involved in co-ordination to iron in the chelate and was the first choice for blocking with the caging group. Salicylaldehyde or pyridoxal was alkylated under basic conditions with 1-(1-bromo-ethyl)-2-nitro-benzene (or benzyl bromide). Condensation of the appropriate aldehydes with isonicotinic acid hydrazide provided the respective Schiff bases in good yield. Spectrophotometric titration (Avramovici-Grisaru *et al.*, 1983) confirmed that all compounds that displayed a blocked or deleted phenol did not bind to iron (data not shown). The efficiency of *in vitro* decaging under physiologically relevant doses of UVA-irradiation was examined for 2-NPE-SIH using high performance liquid chromatography (Figure 2). This confirmed that decaging was efficient at these wavelengths, providing clean conversion to the parent compound.

Cell biology: determination of basal and UVA-induced LIP levels in the primary fibroblast cell line FEK4

The IRP-1/IRE RNA bandshift assay (see, Henderson *et al.*, 1996) was used to estimate the intracellular basal level of LIP

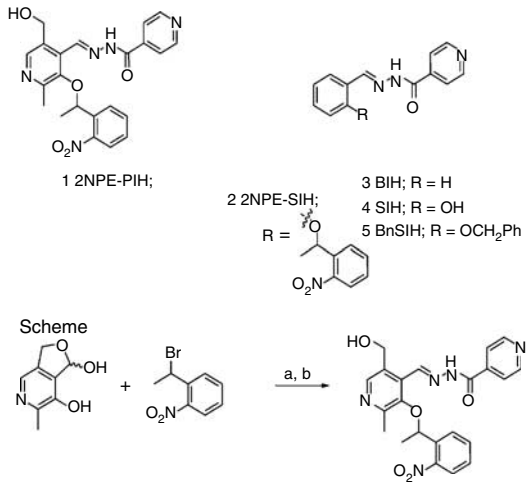

Figure 1. Structures of caged iron chelators and control compounds. (**a**) Cs_2CO_3, DMF; (**b**) isonicotinic acid hydrazide, Dowex® 50WX4-50, $EtOH/H_2O$ (9:1).

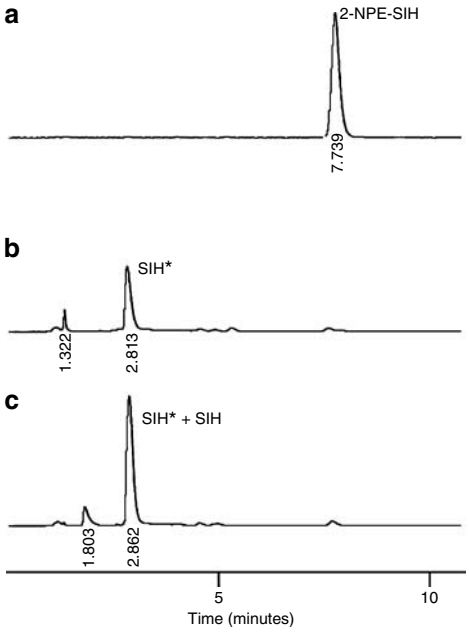

Figure 2. HPLC comparison of SIH and 2-NPE-SIH. (**a**) 2-NPE-SIH (0.1 mm in CH_3CN/aq 1:1); (**b**) same sample after irradiation with 250kJ/m^2 UVA; and (**c**) irradiated sample with SIH co-injection.

in cells treated with either DFO (i.e. positive control) or a series of freshly synthesized compounds 1–5 (Figure 1), namely iron chelators SIH and PIH and their respective caged analogues 2-NPE-SIH and 2-NPE-PIH and BIH (Benzaldehyde isonicotinoyl hydrazone, see, Buss *et al.*, 2003b) and BnSIH ((isonicotinic acid (2-benzyloxy-benzylidene)-hydrazide)) as non-chelating analogues. Flow cytometry revealed that treatment of cells with any of the compounds for 18 hours at 37°C was not toxic up to a final concentration of 250 μM (data not shown). The minimum effective concentration of SIH and PIH was found to be 20 μM, as this was sufficient to activate IRP-1 even at short incubation period (i.e. 30 minutes, data not shown). Figure 3 represents an example of IRP1-IRE bandshift assay carried out with cells treated with 100 μM of the compounds for 18 hours. The treatment of cells with SIH, PIH, and DFO strongly activated the IRP-1-binding activity in response to iron chelation. Modifying the phenolic iron-binding site of SIH in BnSIH, or depleting its phenol moiety in BIH, completely abolished the IRP-1 activation to untreated control levels. Most importantly, cells treated with SIH and PIH elaborated with the 2-NPE caging group (i.e. caged compounds) showed unchanged basal IRP-1 activity, confirming that 2-NPE caging groups are capable of efficiently masking the iron-binding sites of both PIH and SIH chelators.

The calcein (CA) assay was then used to investigate these compounds pre- and post-UVA-irradiation with respect to modulating the intracellular levels of LIP. Cells were treated with individual compounds (20–250 μM) for a total of between 15 minutes and 18 hours, and then irradiated with a UVA dose of 250 kJ/m^2 equivalent to 70 minutes sunlight exposure on a summer day around noon at northern latitude of 30–35° (Frederick and Lubin, 1988). Table 1 provides an example of the CA assays carried out immediately after UVA-irradiation of cells pretreated for 18 hours with compounds at a final concentration of 100 μM. These data, in agreement with that of IRP-1/IRE bandshift assay (see Figure 3), illustrate that sham irradiation of analogues lacking an effective iron-binding site, that is, BIH and BnSIH and the caged compounds 2-NPE-SIH or 2-NPE-PIH, failed to modulate the basal level concentrations of LIP in FEK4 fibroblasts. UVA-induced rises in intracellular LIP was only observed for BIH- and BnSIH-treated cells, consistent with the notion that these compounds are not capable of chelating labile iron. As true time controls, both SIH and PIH were added to irradiation medium for the duration of radiation treatment. This was thought to mimic the time necessary for the caged compounds to be uncaged upon radiation treatment so that they acquire the ability to chelate iron. Our data demonstrated that unlike caged compounds, the addition of PIH or SIH either for duration of irradiation or 18 hours (not shown) led to complete depletion of both basal and UVA-induced LIP (see Tables 1 and 2).

UVA-irradiation of caged-SIH- or caged-PIH-treated cells revealed a significant reduction in the UVA-induced increase in LIP (i.e. to control levels) when compared to the corresponding UVA-irradiated samples. The latter result strongly

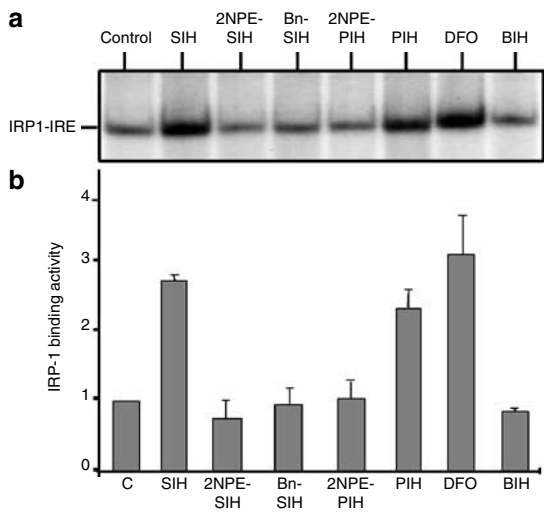

Figure 3. Effect of SIH, PIH, and its derivatives on modulation of IRP1-binding activity in FEK4 fibroblasts. Cells were first treated (or not, for Control) for 18 hours with 100 μM of compounds PIH, SIH, BIH, BnSIH, 3-NPE-SIH, 2-NPE-PIH, and DFO. (**a**) Next, the intracellular level of LIP was estimated by IRP-1-IRE bandshift assay. (**b**) The IRP/IRE signals were then quantified and their relative intensities normalised against that of untreated "Control" cells and then expressed as a fold increase in IRP-1 binding activity above control value.

Table 1. Modulation of LIP levels following irradiation of fibroblasts with UVA

FEK4 condition	[LIP] μM
Control	0.97 ± 0.45
+UVA	2.46 ± 0.67*
BIH	0.97 ± 0.11
BIH+UVA	1.92 ± 0.09*
BnSIH	1.01 ± 0.19
BnSIH+UVA	2.05 ± 0.31*
2-NPE-SIH	0.98 ± 0.12
2-NPE-SIH+UVA	0.95 ± 0.23
2-NPE-PIH	0.94 ± 0.26
2-NPE-PIH+UVA	1.06 ± 0.33
SIH	0
SIH+UVA	0
PIH	0
PIH+UVA	0
DFO	0
DFO+UVA	0

Note: Cells were first treated with compounds (100 μM) for 18 h (except PIH and SIH that were added to the irradiation medium for the duration of irradiation, that is, 15 min) and then irradiated (or sham irradiated) with a UVA dose of 250 kJ/m^2. Measurements were performed in both sham-irradiated and UVA-irradiated samples (i.e. +UVA) immediately after radiation treatment. K_d of CA-Fe for FEK4 was 12.7.The concentrations of LIP are expressed as means ± SD, n=5–7.
*Significantly different from sham-irradiated control, $P<0.05$.

Table 2. Time course of intracellular LIP levels in FEK4 cells following irradiation of fibroblasts with UVA

Time post-UVA (h)	LIP (μM) control	LIP (μM) UVA	LIP (μM) 2-NPE-PIH	LIP (μM) NPE-PIH+UVA	LIP (μM) PIH	LIP (μM) PIH+UVA
0	0.97±0.45	2.46±0.67*	0.94±0.26	1.06± 0.33	0	0
1	0.99±0.18	1.72±0.19*	0.91±0.20	0	0	0
2	0.92±0.14	1.47±0.28*	0.88±0.35	0	0	0
4	0.95±0.23	1.22±0.27	0.93±0.31	0	0	0
6	0.96±0.33	0.92±0.16	0.90±0.21	0	0	0
18	0.94±0.37	0.89±0.29	0.95±0.38	0	0	0

Note: Cells were first treated with compounds for 18 h (except PIH that was added to the irradiation medium for the duration of irradiation time, that is, 15 min) and then irradiated (or sham-irradiated) with a UVA dose of 250 kJ/m^2. Measurements were performed in both sham-irradiated and UVA-irradiated samples (i.e. +UV) at indicated times after radiation treatment. K_d of CA-Fe for FEK4 was 12.7. The concentrations of LIP are expressed as means±SD, n=5–7.
*Significantly different from the corresponding sham-irradiated control, $P<0.05$.

suggests that UVA-irradiation is responsible for photolytic release of either SIH or PIH, which subsequently remove excess labile iron by chelation and transport. Intracellular LIP levels for caged-compound-treated cells were re-examined up to 18 hours following radiation treatment. Sham-irradiated cells treated with caged compounds did not show modulation of basal LIP levels, whereas the equivalent UVA-irradiated population treated with caged compounds apparently continued to show a decrease in the intracellular LIP level because from 1 hour post-irradiation time onwards no intracellular labile iron was detectable (see the example of 2-NPE-PIH in Table 2). A similar time-dependent increase in the binding activity of IRP-1 activity was also observed for the equivalent IRP-1/IRE RNA bandshift assays (data not shown).

Finally, 2-NPE-PIH-treated cells were challenged with hydrogen peroxide, which is also known to cause oxidative damage via an increase in labile iron immediately following oxidizing insult in FEK4 cells (unpublished data, this laboratory). That an increase in labile iron occurred to the same extent in either untreated control cells, or those subject to 2-NPE-PIH is consistent with the notion that UVA-irradiation leads to ablation of the caging group, whereas treatment with hydrogen peroxide does not, so that iron removal observed upon photolysis is likely owing to chelation and transport by the PIH photoproduct (see Table 3).

Table 3. Modulation of LIP levels following treatment of fibroblasts with H_2O_2

FEK4 condition	[LIP]μM
Control	1.17±0.19
100 μM H_2O_2	1.90±0.08*
2-NPE-PIH	0.82±0.09
2-NPE-PIH+100 μM H_2O_2	2.26±0.60*
PIH	0
PIH+100 μM H_2O_2	0

Note: Cells were first treated with compounds (100 μM) for 18 h (except PIH that was added to the serum-free medium for the duration of H_2O_2 treatment, that is, 30 min) and then treated (or sham-treated) with H_2O_2 at a final concentration of 100 μM. Measurements were performed immediately after radiation treatment. K_d of CA-Fe for FEK4 was 12.7.The concentrations of LIP are expressed as means±SD, n=3.
*Significantly different from sham-irradiated control, $P<0.05$.

Determination of the level of UVA-mediated cell death in fibroblasts following treatment with the synthesized compounds

Recent studies in our laboratory have provided a strong link between the level of UVA-induced labile iron release and the extent of necrotic cell death in human skin fibroblasts (Zhong *et al.*, 2004). Furthermore, it was demonstrated that pretreatment of fibroblasts with strong iron chelator DFO significantly decreases the level of UVA-induced necrotic cell death. Based on these findings, we hypothesized that strong iron chelators such as SIH and PIH that also abolish the intracellular LIP should provide protection against UVA-induced necrotic cell death. On the other hand, control compounds BIH and BnSIH that lack iron-binding site should have no protective effect. Additionally, the caged-chelators that are only competent after UVA-irradiation (see Tables 1 and 2, and data not shown) should protect against UVA-induced cell death. For this purpose, FEK4 fibroblasts were treated for 18 hours with a range of concentrations of SIH, PIH, BnSIH, BIH, 2-NPE-SIH, and 2-NPE-PIH (i.e. 20–250 μM) and then the percentage of apoptotic and necrotic cells in UVA-irradiated fibroblasts were scored by flow cytometry using the dual propidium iodide (PI) uptake/Annexin V-FITC binding assay (see Figures 4 and 5) and confirmed by the Apoglow assay that monitors the immediate depletion of intracellular ATP, a recognized hallmark of necrotic cell death (data not shown) (see, Egushi *et al.*, 1997; Leist *et al.*, 1997; Ha and Snyder, 1999; Zhong *et al.*, 2004). In agreement with our previous studies (Pourzand and Tyrrell, 1999; Zhong *et al.*, 2004), UVA induced a dose-dependent increase in necrotic cell death (Figure 4) and the fibroblast cells remained fairly resistant to UVA-induced apoptosis (data not shown). Both SIH and PIH were effective in decreasing the UVA-induced necrotic cell death over the concentration range of 20–250 μM, although optimum protection was observed from 100 μM onwards (e.g. Figure 4a and b). In addition,

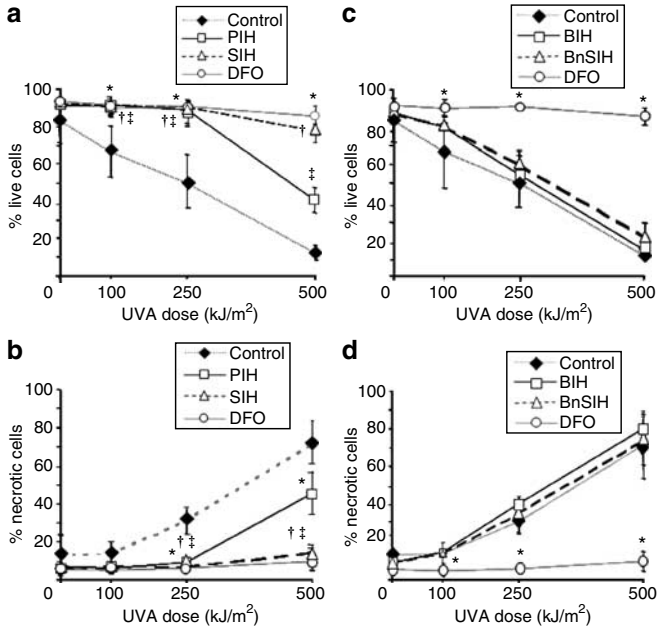

Figure 4. Effect of iron chelators SIH, PIH, and its derivatives on the percentage of necrosis following UVA-irradiation of fibroblasts. (**a**) Percentage live cells for Control and PIH-, SIH-, and DFO-treated cells. (**b**) The corresponding percentage of necrotic cells. (**c**) Percentage live cells for Control and BIH-, BnSIH-, and DFO-treated cells. (**d**) The corresponding percentage of necrotic cells. Cells were first treated (or not, for ''Control'') for 18 hours with 100 μM of compounds PIH, SIH, BIH, BnSIH, and DFO. Next, the percentage of necrotic cell death was scored by flow cytometry 4 hours following irradiation of cells with UVA doses of 0, 100, 250, and 500 kJ/m^2. Values are means $\pm$ SD ($n = 4$–8). *, †, ‡Significantly different from the corresponding irradiated control, $P < 0.05$.

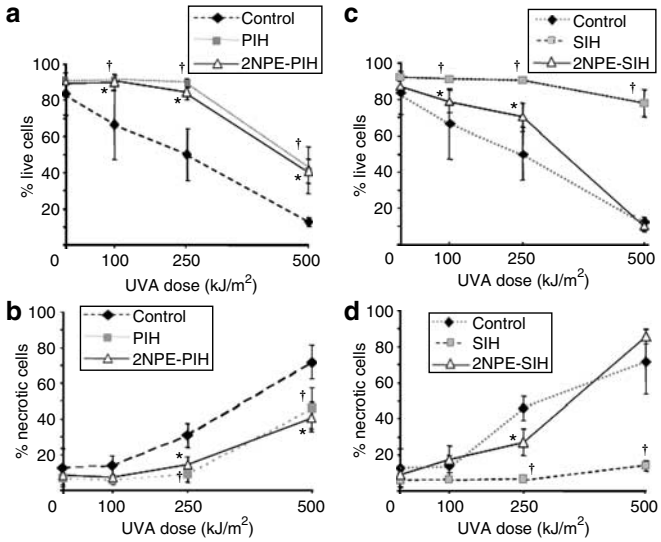

Figure 5. Effect of caged compounds 2NPE-SIH and 2-NPE-PIH on the percentage of necrosis following UVA-irradiation of fibroblasts. (**a**) Percentage live cells for Control and PIH- and 2-NPE-PIH-treated cells. (**b**) The corresponding percentage of necrotic cells. (**c**) Percentage live cells for Control and SIH- and 2-NPE-SIH-treated cells. (**d**) The corresponding percentage of necrotic cells. Cells were first treated (or not, that is, ''Control'') for 18 hours with 100 μM of compounds PIH, SIH, 2-NPE-PIH, and 2-NPE-SIH. Next, the percentage of necrotic cell death was scored by flow cytometry 4 hours following irradiation of cells with UVA doses of 0, 100, 250, and 500 kJ/m^2. Values are means $\pm$ SD ($n = 4$–8). *, †, ‡Significantly different from the corresponding irradiated control, $P < 0.05$.

neither BIH nor BnSIH treatment afforded protection against UVA-induced cell death; the percentage of live cells in FEK4 cells remained unchanged when compared to the corresponding UVA-irradiated control cells (Figure 4c).

At a moderate UVA dose of 250 kJ/m^2, caged compounds 2-NPE-SIH and 2-NPE-PIH showed protection against UVA-induced necrotic cell death over the range of 50–250 μM, but the most effective protection was observed from final concentrations of 100 μM onwards (e.g. Figure 5). At a high dose of 500 kJ/m^2, only 2-NPE-PIH sustained its protective effect against UVA-induced necrotic cell death (Figure 5a–d).

DISCUSSION

Our previous studies clearly demonstrate that exposure of human skin fibroblasts and keratinocytes to UVA component of sunlight promotes the immediate release of potentially harmful labile iron in the cells. Further investigations show that the immediate labile iron release following UVA-irradiation originates mostly from iron liberated from the Ft-bound pool following proteolytic degradation by lysosomal proteases released from damaged lysosomal organelles (Pourzand *et al.*, 1999). Absence of this critical iron storage protein during the first hours following irradiation further exacerbates the consequences of such iron release within human skin cells, as the highly reactive LIP cannot be controlled. Indeed, the increase in LIP is sustained for at least 2 hour following irradiation and only returns to basal levels after 4–6 hours (Table 2 this study and Pourzand *et al.*, 1999; Reelfs *et al.*, 2004; Zhong *et al.*, 2004). This timing coincides with Ft biosynthesis (Pourzand *et al.*, 1999). The prolonged presence of excess labile iron acts to increase dramatically the level of UVA-induced oxidative damage to lysosomal, mitochondrial, and plasma membrane (see, Zhong *et al.*, 2004 and unpublished data, this laboratory). Whereas low UVA doses up to 150 kJ/m^2 appear to cause reversible labile-iron-induced oxidative damage, higher doses of radiation causes cells to undergo necrotic cell death, presumably as a result of severe irreversible damage to its components (see, Pourzand *et al.*, 1999; Pourzand and Tyrrell, 1999 and Figure 4 of this study).

The direct link between UVA-induced iron release and cytotoxicity suggests pathways of protection through iron chelation. Previous studies from this laboratory demonstrated that DFO treatment can substantially protect both cultured skin fibroblasts and keratinocytes against UVA-mediated membrane damage and necrotic cell death by depleting the potentially harmful labile iron present in the cells (Pourzand *et al.*, 1999; Reelfs *et al.*, 2004; Zhong *et al.*, 2004). While tempting to propose that strong chelators such as DFO can be used as sunscreens additives, several studies link prolonged exposure to iron chelators with deleterious side effects on cells, tissues, and organs owing to systemic iron depletion (e.g. Porter and Huens, 1989; Simonart *et al.*, 2002).

Herein, we describe a new strategy based on caged-iron chelators that only release the active compound on exposure to physiologically relevant doses of UVA-irradiation. Ideally, such caged compounds should have (i) high lipophilicity to enter easily the cells; (ii) low toxicity; (iii) no iron-chelation property under normal conditions and high affinity for iron upon UVA-irradiation; (iv) no toxic photo-by-products released upon uncaging; (v) and most important, have highly protective effect against UVA-induced damage and cytotoxicity. The lipophilic strong chelators SIH and PIH were used to develop prototype caged compounds using the well-studied ortho-nitrobenzyl derivatives (Kaplan *et al.*, 1978). Our data indicate that both caged compounds are sufficiently lipophilic to enter cells and tissues, display low affinity for iron and no cytotoxicity and are therefore dispersed within skin cells, without eliciting harmful side effects such as prolonged iron starvation. Exposure of cells treated with the prototype compounds to UVA light yields highly potent iron chelators SIH and PIH that efficiently decrease the resulting labile iron immediately following radiation treatment. Most importantly, this effect coincides with a reciprocal decrease in the percentage of necrotic cell death. Cells treated with either caged compounds were significantly protected against UVA-induced necrotic cell death at a moderate UVA dose of 250 kJ/m^2 (i.e. at natural exposure levels). At a UVA higher dose of 500 kJ/m^2, only 2-NPE-PIH-treated cells exhibit protection against UVA-induced necrotic cell death. Furthermore, as it can be seen in Figure 5b, the decrease in the necrotic cell population for both PIH- and 2-NPE-PIH-treated cells were almost identical for all the UVA doses used, indicating that UVA converts 2-NPE-PIH to PIH. Additionally, the photo-by-products of 2-NPE-PIH appear to have low toxicity to the cells during the study period. Clearly, neither the long-term administration of nitroaromatics nor the fact that 2-nitrosobenzoyl photolysis products may undergo potentially cytotoxic reaction with amines support the long-term utility of these prototype compounds. Exploration of more benign caging groups is anticipated as an essential future development for the project.

2-NPE-SIH is only partially protective even at low to moderate doses of UVA when compared to SIH, and not protective at the high dose of 500 kJ/m^2. The reason for this is not clear, but one possible explanation is that the intracellular localization of 2-NPE-SIH and 2-NPE-PIH are different and that decaging is therefore less efficient, or that the photo-products are harmful to cells, or themselves incapable of iron chelation. In a related unpublished study from this laboratory, we observed that unlike 2-NPE-PIH, PIH, and SIH, the caged compound 2-NPE-SIH shows significant toxicity to lysosomal membranes following irradiation of FEK4 cells with a high UVA dose of 500 kJ/m^2.

2-NPE-PIH provides demonstration of a novel concept for the protection of skin cells against prolonged exposure to sunlight. Whether this compound can be considered as a potential sunscreen component requires further *in vivo* studies and optimization and exploration of other caging groups and iron chelators. At present, there are no caged probes for iron available and the molecules that we have synthesized may provide a useful addition to the arsenal of chemical sensors available for biological studies. While photodynamic therapy is well known (Dolmans *et al.*, 2003) and the methods for delivering light to target areas well developed, there are very relatively few examples of prodrugs activated by photolysis. This present study may invigorate efforts in this area, although modulation of targeting and the wavelength of release are anticipated here.

In summary, we describe here a totally different way of approaching the protection of cells from UV damage. Although the techniques of chelation and caging used here are familiar, their combination and application in a completely novel arena make the target compounds very innovative.

MATERIALS AND METHODS

Chemistry: synthesis of 2-NPE-SIH and 2-NPE-PIH – general

All solvents and reagents were purchased from commercial sources and used as received. ^{1}H and ^{13}C NMR (nuclear magnetic resonance) were obtained on a Varian EX-400 NMR spectrometer at 400 and 100 MHz, respectively. Mass spectra were recorded at University of Bath Mass Spectrometry Service on a VG Analytical Autospec Mass Spectrometer using fast atom bombardment (FAB) with 3-nitrobenzyl alcohol as a matrix. Elemental analysis was performed at the University of Bath Service. Melting points were determined using a Reichtert-Jung Therm Galen Kofler block and are uncorrected. Reverse-phase high performance liquid chromatography analysis was performed on Varian Dynamax model SD-200 using a reverse-phase column (Kingsorb C18, 5 μm, 150 × 4.60 mm, Phenomenex, Macclesfield Cheshire, UK) using isocratic elution with 50% CH_3CN–50% water with UV detection set at 282 nm.

General procedure for phenol alkylation. A solution of the phenol (2.5 mmol), 1-(1-bromo-ethyl)-2-nitro-benzene, and Cs_2CO_3 in dimethyl formamide was stirred at 60°C for 12 hours, then concentrated under vacuum. The resulting crude was dissolved into ethyl acetate, washed with 2 M aqueous NaOH, then brine and the organics dried over sodium sulfate, dried and concentrated.

2-[1-(2-Nitrophenyl)ethoxy]benzaldehyde. ^{1}H-NMR (400 MHz, $CDCl_3$) δ1.77 (3H, d, *J* 6.3 Hz, CH_3), 6.16 (1H, q, *J* 6.3 Hz, $CHCH_3$), 6.69 (1H, d, *J* 7.8 Hz, ArH), 6.98 (1H, t, *J* 7.8 Hz, ArH), 7.37 (1H, dt, *J* 7.8, 1.7 Hz, ArH), 7.45 (1H, dt, *J* 7.9, 1.4 Hz, ArH), 7.62 (1H, dt, *J* 7.9, 1.4 Hz, ArH), 7.77 (1H, dd, *J* 7.9, 1.4 Hz, ArH), 7.82 (1H, dd, *J* 7.8, 1.7 Hz, ArH), 8.04 (1H, dd, *J* 7.9, 1.4 Hz, ArH), 10.64 (1H, s, CHO); ^{1}H-NMR (100 MHz, $CDCl_3$) 23.5, 72.1, 113.6, 121.3, 124.9, 125.3, 127.4, 128.7, 128.8, 134.4, 136.0, 138.2, 159.5, 189.6; and *m/z* (FAB$^+$) 272.0927 (M + H, for $C_{15}H_{14}NO_4$ required 272.0923).

6-Methyl-7-[1-(2-nitrophenyl)ethoxy]-1,3-dihydrofuro[3,4-c]pyridin-1-ol. Chromatography on silica gel using ethyl acetate: hexane (7:3) as eluent and recrystallization from ethyl acetate: hexane gave the product as a beige powder. Mp 163–165°C; two diastereoisomers A:B 6:4; ^{1}H-NMR (400 MHz, $CDCl_3$) A: δ1.73 (3H, d, *J* 6.3, CH_3CH), 2.60 (3H, s, CH_3Py), 4.19 (1H, brs, O*H*), 4.90 (1H, d, *J* 12.7 Hz, CH_aH_b), 5.19 (1H, d, *J* 12.7 Hz, CH_aH_b), 6.14 (1H, s, C*H*OH), 6.35 (1H, q, *J* 6.3 Hz, $CHCH_3$), 7.46 (1H, dt, *J* 8.0, 1.3 Hz, Ar*H*), 7.67 (1H, dt, *J* 8.0, 1.3 Hz, Ar*H*), 7.84 (1H, dd, *J* 8.0, 1.3 Hz,

ArH), 8.01 (1H, dd, *J* 8.0, 1.3 Hz, ArH), 8.05 (1H, s, PyH); B: 1.72 (3H, d, *J* 6.3 Hz, CH_3CH), 2.58 (3H, s, CH_3Py), 4.19 (1H, brs, OH), 4.99 (1H, d, *J* 12.7 Hz, CH_aH_b), 5.20 (1H, d, *J* 12.7 Hz, CH_aH_b), 6.22 (1H, q, *J* 6.3 Hz, $CHCH_3$), 6.55 (1H, s, CHOH), 7.46 (1H, dt, *J* 8.0, 1.3 Hz, ArH), 7.72 (1H, dt, *J* 8.0, 1.3 Hz, ArH), 7.96 (1H, dd, *J* 8.0, 1.3 Hz, ArH), 8.04 (1H, dd, *J* 8.0, 1.3 Hz, ArH), 8.07 (1H, s, PyH); ^{13}C NMR (100 MHz, $CDCl_3$) (two diastereoisomers): δ19.8, 19.9, 23.6, 23.9, 69.6, 69.7, 74.8, 75.6, 99.6, 99.7, 124.5, 124.9, 127.4, 127.9, 128.5, 128.6, 133.9, 134.1, 135.0, 135.1, 135.3, 135.4, 135.7, 135.8, 139.1, 147.0, 147.1, 147.2, 150.2, 150.4; HRMS (FAB+) calcd. for $C_{16}H_{17}N_2O_5$ 317.1137 (M+H); found 317.11404 (M+H); anal. calcd. $C_{16}H_{16}N_2O_5$: C, 60.75, H, 5.10, N, 8.86; found: C, 60.40, H, 5.08, N, 8.93.

General procedure for hydrazide formation. A solution of aldehyde (**6**, or **7**, 1 mmol,) and isonicotinic acid hydrazide (1 mmol) in ethanol:water (9:1, 10 ml) was heated at reflux for 24 hours.

Isonicotinic acid [1-{5-hydroxymethyl-2-methyl-[1-(2-nitrophenyl)-ethoxy]-pyridin-4-yl}-meth-(E)-ylidene]-hydrazide 2. Obtained as a white precipitate from the cooled reaction mixture, 82%. mp 227–229°C; ^{1}H-NMR (400 MHz, $(CD_3)_2SO$, Me_4Si) 1.73 (3H, d, *J* 6.2 Hz, CH_3), 6.09 (1H, q, *J* 6.2 Hz, CHO), 6.85 (1H, d, *J* 7.9 Hz, ArH), 7.01 (1H, t, 7.9 Hz, ArH), 7.30, (1H, dt, *J* 7.9, 1.7 Hz, ArH), 7.60 (1H, dt, *J* 7.2, 1.7 Hz, ArH), 7.67–7.82 (2H, m, ArH), 7.88 (2H, d, *J* 6.1 Hz, PyH), 7.91 (1H, dd, *J* 7.9, 1.7 Hz, ArH), 8.08 (1H, dd, *J* 7.2, 1.7 Hz, ArH), 8.82 (2H, d, *J* 6.1 Hz, PyH), 8.37 (1H, s, CHN), 12.17 (1H, s, NH); ^{13}C NMR (100 MHz, $(CD_3)_2SO$, Me_4Si) 23.3, 71.7, 114.2, 121.9, 122.1, 123.4, 125.2, 126.5, 127.7, 129.7, 132.2, 134.8, 137.5, 141.1, 144.7, 148.0, 150.8, 155.8, 162.0; HRMS (FAB) calcd. for $C_{21}H_{19}N_4O_4$: 391.14063 (M+H); found 391.14207 (M+H); anal. calcd. $C_{21}H_{18}N_4O_4$: C, 64.61, H, 4.65, N, 14.35; found: C, 64.60, H, 4.68, N, 14.30.

Isonicotinic acid [1-{5-hydroxymethyl-2-methyl-3-[1-(2-nitrophenyl)-ethoxy]-pyridin-4-yl}-meth-(E)-ylidene]-hydrazide 1. Reaction performed in presence of Dowex® 50WX4-50 acidic resin, filtered, and concentrated reaction mixture was purified by column chromatography on silica gel eluting from 0.5:99.0 methanol and dichloromethane to 5.0:95.0, then recrystallized from ethyl acetate/ethanol to afford the title compound as a white powder, 65%. Mp 191–193°C; ^{1}H-NMR (400 MHz, $(CD_3)_2SO$) 1.63 (3H, d, *J* 6.2 Hz, CH_3CHO), 2.36 (3H, s, CH_3Py), 4.66 (2H, d, *J* 6.3 Hz, CH_2OH), 5.28 (1H, t, *J* 6.3 Hz, OH), 5.50 (1H, q, *J* 6.2 Hz, CHO), 7.61 (1H, dt, *J* 7.9 Hz, 1.2, ArH), 7.83 (2H, d, *J* 5.9 Hz, PyH), 7.87 (1H, dt, *J* 7.9, 1.2 Hz, ArH), 7.96 (1H, dd, *J* 7.9, 1.2 Hz, ArH), 8.11 (1H, dd, *J* 7.9, 1.2 Hz, ArH), 8.43 (1H, s, CHN), 8.66 (1H, s, PyH), 8.84 (2H, d, *J* 5.9 Hz, PyH), 12.38 (1H, s, NH); ^{13}C NMR (100 MHz, $(CD_3)_2SO$) 20.1, 22.4, 60.5, 77.4, 122.0, 124.6, 129.2, 129.9, 132.7, 134.27, 134.33, 136.2, 140.4, 144.3, 144.7, 148.0, 150.3, 151.0, 152.0, 162.6; HRMS (FAB) calcd. for $C_{22}H_{22}N_5O_5$: 436.16209 (M+H); found 436.16073 (M+H); Anal. calcd. $C_{22}H_{21}N_5O_5$: C 60.68, H 4.86, N 16.08; found: C 60.60, H 4.86, N 16.00.

Cell biology

The medical ethical committee of the University of Bath approved all described studies. The study was conducted according to The Declaration of Helsinki Principles.

Chemicals. All the Cell biology reagents were from Sigma Chemical (St-Louis, MO), except Annexin V (Roche, Lewes, UK), DFO (Desferal from Novartis, Basel, Switzerland), CA-AM (calcein-acetoxymethyl ester; Molecular Probes, Eugene, OR), and Apoglow kit reagents (Lumitech, Nottingham, UK). Cell culture materials were from Life Technologies (Paisley, Scotland), except fetal calf serum (PAA Laboratories, Teddington, UK) and phosphate-buffered saline (Oxoid Basingstoke, UK). Stock solutions were prepared in phosphate-buffered saline, except DFO and PI in water, PIH (Baker et al., 1992) in 1 N HCl, and SIH (Baker *et al.*, 1992), 2NPE-SIH, and 2-NPE-PIH in DMSO. Final concentration of DMSO in the medium did not exceed 0.2%. The water used to prepare solutions was from a MilliQ purification system (Millipore, Bedford, MA) in order to minimize the presence of trace elements such as transition metals.

Cell culture. The human fibroblast cell line FEK4 (kindly provided by R. M. Tyrrell, Bath University, UK) was derived from newborn foreskin explants (Zhong *et al.*, 2004). Fibroblast (3.5×10^5; passages 12–14) monolayers were grown in 10 cm dishes for 3–4 days in order to reach 80% confluency on the day of the experiment as described previously (Pourzand *et al.*, 1999).

Irradiation. Irradiations were performed in phosphate-buffered saline at approximately 25°C using a broad-spectrum Sellas 4 kW UVA lamp (Sellas, Germany), as described previously (Pourzand *et al.*, 1999). UVA doses were measured using an IL1700 radiometer (International Light, Newbury, MA). Control cells were treated in the same manner, except that they were not irradiated (i.e. sham irradiation).

CA loading and intracellular LIP estimation. The method used to estimate the level of intracellular CA-bound iron (CA-Fe) was modified from Epsztejn *et al.* (1997) as described previously (Pourzand *et al.*, 1999; see, Kakhlon and Cabantchik, 2002). To determine the intracellular level of LIP, which is operationally defined as the sum of the intracellular level of CA-bound iron (i.e. [CA-Fe]) and free iron (i.e. [Fe] unbound to CA), the cell-dependent dissociation constant (K_d) for CA-Fe was obtained as described previously (Zhong *et al.*, 2004). From the K_d value, the absolute intracellular level of free iron (i.e. [Fe] unbound to CA) was then calculated and the results expressed as micromolar concentration of LIP (i.e. [CA-Fe] + [Fe]). When cells were treated with SIH, the dequenching of the CA-Fe was performed with PIH and confirmed with DFO.

Intracellular LIP estimation by IRP/ IRE RNA bandshift assay. To evaluate the modulation of the basal LIP levels in cells treated with various compounds, we employed the IRP/IRE (iron regulatory protein/iron-responsive element) RNA- bandshift assay. In this method, the level of iron is monitored by the formation of complexes between IRP and the IRE of ferritin (Ft) mRNA as described previously (Pourzand *et al.*, 1999; see, Kakhlon and Cabantchik, 2002). Briefly, the cytoplasmic extracts were first prepared at the indicated time following treatment with the compounds according to Müllner *et al.* (1992) and then probed with gel-purified ^{32}P-labeled wild-type (i.e. recognizes both IRP-1 and IRP-2) or IRP-1-specific RNAs (kindly provided by L. Kuhn, Swiss Institute For Experimental Cancer Research, Switzerland; see, Henderson *et al.*, 1996) in the

presence of 5 mg/ml heparin. RNA–protein complexes were resolved on a 6% non-denaturing gel and processed for autoradiography. Quantification of the IRP/IRE signals was carried out with a PhosphorImager (Molecular Dynamics, Sunnyvale, CA) using IMAGEQUANT software 3.3 (National Institutes of Health, Bethesda, MD).

Flow cytometry. The percentage of apoptotic and necrotic cells were scored after dual staining of cells with PI and Annexin V-FITC staining by flow cytometry using the FACS vantage (Becton Dickinson) as described previously (Zhong *et al.*, 2004). Double-stained cells and Annexin V-negative/PI-positive cells were considered ''necrotic'', whereas Annexin V-positive/ PI-negative cells were ''apoptotic''. Annexin V-negative/PI-negative were the ''live'' cells.

Statistical methods. Results are expressed as the mean $\pm$ SD. Significant differences ($P<0.05$) were determined by either paired or unpaired *t*-test after one-way analysis of variance.

CONFLICT OF INTEREST

The authors state no conflict of interest.

ACKNOWLEDGMENTS

We thank Professors L. Kuhn for IRE vectors and P. Ponka for SIH and PIH at the early stages of the study, Professor Rex Tyrrell for FEK4 cell line, the use of UVA lamp, spectrofluorimeter, and luminometer facilities in his laboratory and for useful discussions throughout the study, and Mrs Patricia Holley for her excellent technical assistance. This research was supported by the Wellcome Trust Showcase Award (Contract no. 067653/Z/02/Z).

REFERENCES

Avramovici-Grisaru S, Sarel S, Link G, Hershkof C (1983) Syntheses of iron bis(pyridoxal isonicotinoyl hydrazone)s and the *in vivo* iron-removal properties of some pyridoxal derivatives. *J Med Chem* 26:298–302

Baker E, Richardson D, Gross S, Ponka P (1992) Evaluation of the iron chelation potential of hydrazones of pyridoxal, salicaldehyde and 2-hydroxy-1-naphthylaldehyde using the hepatocyte in culture. *Hepatology* 15:492–501

Beinert H, Kennedy MC (1993) Aconitase, a two faced protein: enzyme and iron regulatory factor. *FASEB J* 7:442–1449

Bisset D, Chaterjee R, Hannon DP (1991) Chronic ultraviolet radiation-induced increase in skin iron and the photoprotective effect of topically applied iron chelators. *Photochem Photobiol* 54:215–23

Breuer W, Epsztejn S, Cabantchik ZI (1996) Dynamics of the cytosolic chelatable iron pool of K562 cells. *FEBS Lett* 382:304–8

Buss JL, Arduini E, Shephard KC, Ponka P (2003a) Lipophilicity of analogs of pyridoxal isonicotinoyl hydrazone (PIH) determines the efflux of iron complexes and toxicity in K562 cells. *Biochem Pharmacol* 65:349–60

Buss JL, Neuzil J, Gelbert N, Weber C, Ponka P (2003b) Pyridoxal isonicotinoyl hydrazone analogs induce apoptosis in hematopoietic cells due to their iron-chelating properties. *Biochem Pharmacol* 65: 161–72

Cairo G, Castrusini E, Minotti G, Bernelli-Zazzera A (1996) Superoxide and hydrogen peroxide-dependent inhibition of iron regulatory protein activity: a protective stratagem against oxidative injury. *FASEB J* 10:1326–35, (comment in: *FASEB J* 1996; 11:374–5)

Cairo G, Pietrangelo A (2000) Iron regulatory proteins in pathobiology. *Biochem J* 352:241–50

Cairo G, Tacchini L, Pogliaghi G, Anzon E, Tomasi A, Bernelli-Zazzera A (1995) Induction of ferritin synthesis by oxidative stress. Transcriptional and post-transcriptional regulation by expansion of the ''free'' iron pool. *J Biol Chem* 270:700–3

Chaston TB, Richardson DR (2003) Iron chelators for the treatment of iron overload disease: relationship between structure, redox activity, and toxicity. *Am J Hematol* 73:200–10

Creighton-Gutteridge M, Tyrrell RM (2002) A novel iron chelator that does not induce HIF-1 activity. *Free Radic Biol Med* 33:356–63

Dolmans DE, Fukumura D, Jain RK (2003) Photodynamic therapy for cancer. *Nat Rev Cancer* 5:380–7

Egushi Y, Shimizu S, Tsujimoto Y (1997) Intracellular ATP levels determine cell death fate by apoptosis or necrosis. *Cancer Res* 57:1835–40

Epsztejn S, Kakhlon O, Glickstein H, Breuer W, Cabantchik I (1997) Fluorescence analysis of the labile iron pool of mammalian cells. *Anal Biochem* 248:31–40

Frederick JE, Lubin D (1988) Possible long-term changes in biologically active ultraviolet radiation reaching the ground. *Photochem Photobiol* 47: 571–8

Galey JB, Destrée O, Dumats J, Génard S, Tachon P (2000) Protection against oxidative damage by iron chelators: effect of lipophilic analogues and prodrugs of *N*, *N*′-bis (3, 4, 5-trimethoxybenzyl) ethylene-diamine *N*, *N*′-diacetic acid (OR10141). *J Med Chem* 43:1418–21

Guo B, Phillips JD, Yu Y, Leibold EA (1995) Iron regulates the intracellular degradation of iron regulatory protein 2 by the proteasome. *J Biol Chem* 270:21645–51

Ha HC, Snyder SH (1999) Poly(ADP-ribose) polymerase is a mediator of necrotic cell death by ATP depletion. *Proc Natl Acad Sci USA* 96: 13978–82

Henderson BR, Menotti E, Kühn LC (1996) Iron regulatory proteins 1 and 2 bind distinct sets of RNA target sequences. *J Biol Chem* 271:4900–8

Hentze MW, Kuhn LC (1996) Molecular control of vertebrate iron metabolism: mRNA based regulatory circuits operated by iron, nitric oxide, and oxidative stress. *Proc Natl Acad Sci USA* 93:8175–82

Hermes-Lima M, Santos NCF, Yan J, Andrews M, Schulman HM, Ponka P (1999) EPR spin trapping and 2-deoxyribose degradation studies of the effect of pyridoxal isonicotinoyl hydrazone (PIH) on *OH formation by the Fenton reaction. *Biochim Biophys Acta* 1426:475–82

Hershko C, Avramovici-Grisaru S, Link G, Gelfand L, Sarel S (1981) Mechanism of *in vivo* iron chelation by pyridoxal isonicotinoyl hydrazone and other imino derivatives of pyridoxal. *J Lab Clin Med* 98:99–108

Hileti D, Panayiotidis P, Hoffbrand AV (1995) Iron chelators induce apoptosis in proliferating cells. *Br J Haematol* 89:181–7

Horackova M, Ponka P, Byczko Z (2000) The antioxidant effects of a novel iron chelator salicylaldehyde isonicotinoyl hydrazone in the prevention of H(2)O(2) injury in adult cardiomyocytes. *Cardiovasc Res* 47:529–36

Huang AR, Ponka P (1983) A study of the mechanism of action of pyridoxal isonicotinoyl hydrazone at the cellular level using reticulocytes loaded with non-heme ^{59}Fe. *Biochim Biophys Acta* 757:306–15

Kakhlon O, Cabantchik ZI (2002) The labile iron pool: characterization, measurement, and participation in cellular processes. *Free Radic Biol Med* 33:1037–46

Kaplan JH, Forbush BIII, Hoffman JF (1978) Rapid photolytic release of adenosine 5′-triphosphate from a protected analogue: utilization by the Na:K pump of human red blood cell ghosts. *Biochemistry* 17:1929–35

Kitazawa M, Ishitsuka Y, Kobayashi M, Nakano T, Iwasaki K, Sakamoto K *et al.* (2005) Protective effects of an antioxidant derived from serine and vitamin B6 on skin photoaging in hairless mice. *Photochem Photobiol* 81:970–4

Klausner RD, Rouault TA, Harford JB (1993) Regulation of the fate of mRNA: the control of cellular iron metabolism. *Cell* 72:19–28

Kuhn LC (1994) Molecular regulation of iron proteins. *Baillieres Clin Haematol* 7:763–85

Kvam E, Hejmadi V, Ryter S, Pourzand C, Tyrrell RM (2000) Heme oxygenase activity causes transient hypersensitivity to oxidative ultraviolet A radiation that depends on release of iron from heme. *Free Radic Biol Med* 28:1191–6

Leist M, Single B, Castoldi AF, Kuhnle S, Nicotera P (1997) Intracellular adenosine triphosphate (ATP) concentration: a switch in the description between apoptosis and necrosis. *J Exp Med* 185:1481–6

Martins EA, Robalinho RL, Meneghini R (1995) Oxidative stress induces activation of a cytosolic protein responsible for control of iron uptake. *Arch Biochem Biophys* 316:128–34

Müllner EW, Rothenberger S, Müller AM, Kühn LC (1992) *In vivo* and *in vitro* modulation of the mRNA-binding activity of iron-regulatory factor. Tissue distribution and effects of cell proliferation, iron levels and redox state. *Eur J Biochem* 208:597–605

Pantopoulos K, Hentze MW (1995) Rapid responses to oxidative stress mediated by iron regulatory protein. *EMBO J* 14:2917–24

Petrat F, de Groot H, Rauen U (2001) Subcellular distribution of chelatable iron: a laser scanning microscopic study in isolated hepatocytes and liver endothelial cells. *Biochem J* 356:61–9

Ponka P, Borova J, Neuwirt J, Fuchs O, Necas E (1979) A study of intracellular iron metabolism using pyridoxal isonicotinoyl hydrazone and other synthetic chelating agents. *Biochim Biophys Acta* 586: 278–97

Ponka P, Richardson DR, Edward JT, Chubb FL (1994) Iron chelators of the pyridoxal isonicotinoyl hydrazone class. Relationship of the lipophilicity of the apochelator to its ability to mobilise iron from reticulocytes *in vitro*. *Can J Physiol Pharmacol* 72:659–66

Porter JB, Huens ER (1989) The toxic effects of desferrioxamine. *Bailliere's Clin Haematol* 2:459–74

Pourzand C, Tyrrell RM (1999) Apoptosis, the role of oxidative stress and the example of solar ultraviolet A radiation. *Photochem Photobiol* 70: 380–90

Pourzand C, Watkin RD, Brown JE, Tyrrell RM (1999) Ultraviolet A radiation induces immediate release of iron in human primary skin fibroblasts: the role of ferritin. *Proc Natl Acad Sci USA* 96:6751–6

Rakba N, Loyer P, Gilot D, Delcros JG, Glaise D, Baret P *et al.* (2000) Antiproliferative and apoptotic effects of O-Trensox, a new synthetic iron chelator, on differentiated human hepatoma cell lines. *Carcinogenesis* 21:943–51

Reelfs O, Tyrrell RM, Pourzand C (2004) Ultraviolet a radiation-induced immediate iron release is a key modulator of the activation of NF-kappa B in human skin fibroblasts. *J Invest Dermatol* 122:1440–7

Richardson DR, Ponka P (1998) Orally effective iron chelators for the treatment of iron overload disease: the case for a further look at pyridoxal isonicotinoyl hydrazone and its analogs. *J Lab Clin Med* 132:351–2, (comment on *J Lab Clin Med* 1998; 131:290–1)

Santos NC, Castilho RF, Meinicke AR, Hermes-Lima M (2001) The iron chelator pyridoxal isonicotinoyl hydrazone inhibits mitochondrial lipid peroxidation induced by Fe(II)-citrate. *Eur J Pharmacol* 428:37–44

Séité S, Popovic E, Verdier MP, Roguet R, Portes P, Cohen C *et al.* (2004) Iron chelation can modulate UVA-induced lipid peroxidation and ferritin expression in human reconstructed epidermis. *Photodermatol Photoimmunol Photochem* 20:47–52

Simonart T, Degraef C, Andrei G, Mosselmans R, Hermans P, Van Vooren JP *et al.* (2002) Desferrioxamine enhances AIDS-associated Kaposi's sarcoma tumor development in a xenograft model. *Int J Cancer* 100: 140–3

Simonart T, Van Vooren JP, Parent D, Heenen M, Boelaert JR (2000) Role of iron in dermatology. *Dermatology* 200:156–9

Šimùnek T, Klimtová I, Kaplanová J, Štìrba M, Mazurová Y, Adamcová M *et al.* (2005) Study of daunorubicin cardiotoxicity prevention with pyridoxal isonicotinoyl hydrazone in rabbits. *Pharmacol Res* 51:223–31

Singh S, Khodr H, Taylor M, Hider RC (1995) Therapeutic iron chelators and their potential side-effects. *Biochem Soc Symp* 61:127–37

Zhong JL, Yiakouvaki A, Holley P, Tyrrell RM, Pourzand C (2004) Susceptibility of skin cells to UVA-induced necrotic cell death reflects the intracellular level of labile iron. *J Invest Dermatol* 123:771–80